Supplementary Materials

Contents

Section S1 Statistical calculation methods of HRTEM

The morphological details of the (Ni)MoS slab were statistically calculated by the published formula[1,2]:

Average slab length:

$$\bar{L} = \sum_{i=1}^{n} n_i l_i \Big/ \sum_{i=1}^{n} n_i \quad \text{(S1)}$$

Average stack number:

$$\bar{N} = \sum_{i=1}^{n} n_i N_i \Big/ \sum_{i=1}^{n} n_i \quad \text{(S2)}$$

In Eq.(S1) and Eq.(S2), the length and stacking number of slab i are represented by l_i and N_i, respectively, while the number of (Ni)MoS_2 slabs whose length is l_i is represented by n_i. The dispersion degrees of Mo species (D_{Mo}) were calculated by Eq.(S3)[3,4]:

$$D_{Mo} = Mo_e \Big/ Mo_t = \sum_{i=1}^{t} 6(n_i - 1) \Big/ \sum_{i=1}^{t} (3n_i^2 - 3n_i + 1) \quad \text{(S3)}$$

In Eq. (S3), the number of Mo atoms at the edge locations and the total number of Mo atoms in the MoS_2 slabs are represented by Mo_e and Mo_t, respectively; n_i is the number of Mo atoms alongside one edge of the MoS_2 slab, as determined by the length ($l_i = 3.2(2n_i - 1)\dot{A}$) and t stands the statistical number of MoS_2 slabs.

Figure S1 Raman spectra of the synthesized catalysts

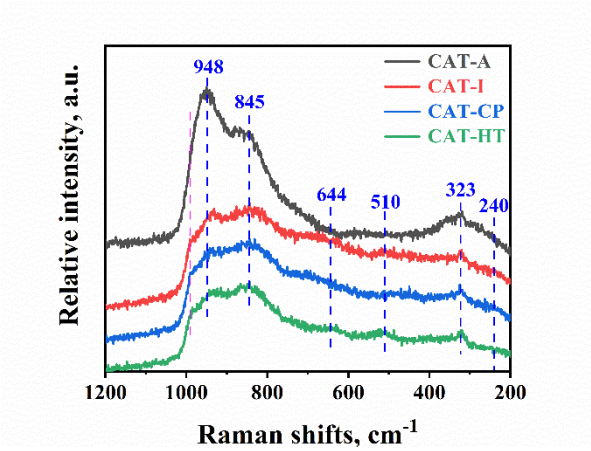

Figure S1. Raman spectra of the synthesized catalysts.

To further confirm the states of the Mo species over the synthesized catalysts, Raman characterization was performed, and the recorded spectra are displayed in Figure S1. Peaks at 948 cm^{-1} are assigned to the symmetric Mo=O terminal stretches of $Mo_7O_{24}^{6-}$ species, and these Mo oxide species are considered to have a weak MSI[5]. Peaks centered around 845 and 323 cm^{-1} are due to the stretching and bending vibration of Mo=O in tetrahedrally coordinated molybdate like MoO_4^{2-}, which has strong MSI[6]. Bands at 644 and 510 cm^{-1} are assigned to the typical anatase phase[7].

It can be concluded from Figure S1 that the intensity of the peaks at 948cm^{-1} and 845cm^{-1} of titanium-containing catalysts do not have a significant variation. In other words, the formation of tetrahedrally coordinated molybdate has been facilitated in titanium-containing catalysts. Additionally, with the incorporation of titania, the Raman band assigned to the polymolybdenum shifts to a higher frequency. The increase of the Raman shifts not only indicates the progressively higher degree of polymerization of Mo anions[8,9] but also indicates the stronger MSI[10]. In such a case, large polymolybdenum clusters were formed but avoided MoO_3 formation, which could be verified from the XRD catalyst patterns of Figure S2.

Moreover, for titanium-containing catalysts, the diffraction peak was relatively broad at 890-1000cm^{-1}, which has been overlapped with the Mo=O stretching vibrations at 948cm^{-1}. The broad feature of this peak indicated the existence of a well-dispersed amorphous phase of MoO_x on the TiO_2-Al_2O_3 support surface[11].

Figure S2 Wide-angle XRD patterns of the synthesized catalysts

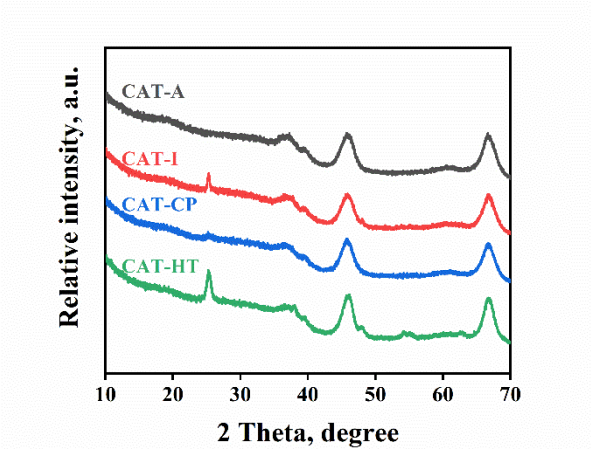

Figure S2. Wide-angle XRD patterns of the synthesized catalysts.

XRD characterization methods have also been used to evaluate the dispersion of active metals on the supports. The orthorhombic MoO_3 characteristic peaks are identified at 2θ of 13°, 23.42°, 26°, 27.52°, and 39° (JCPDS card no. 05-0508), whereas the anatase peaks are identified at 2θ of 26°, 39° and 67°. As shown in Figure S2, the intensity of all diffraction peaks of synthesized catalysts, especially anatase characteristic peaks, is similar to the pure supports, indicating that MoO_3 is well-dispersed on the supports.

References

1. Topsøe, H.; Clausen, B.S. Importance of Co-Mo-S Type Structures in Hydrodesulfurization. *Catalysis Reviews* **1984**, *26*, 395–420, doi:10.1080/01614948408064719.
2. [2] Zhang, P.; Mu, F.; Zhou, Y.; Long, Y.; Wei, Q.; Liu, X.; You, Q.; Shan, Y.; Zhou, W. Synthesis of Highly Ordered TiO_2-Al_2O_3 and Catalytic Performance of Its Supported NiMo for HDS of 4, 6-Dimethyldibenzothiophene. *Catalysis Today* **2020**, *423*, 112716, doi:10.1016/j.cattod.2020.03.003.
3. [3] Nikulshin, P.A.; Salnikov, V.A.; Mozhaev, A.V.; Minaev, P.P.; Kogan, V.M.; Pimerzin, A.A. Relationship between Active Phase Morphology and Catalytic Properties of the Carbon–Alumina-Supported Co(Ni)Mo Catalysts in HDS and HYD Reactions. *Journal of Catalysis* **2014**, *309*, 386–396, doi:10.1016/j.jcat.2013.10.020.
4. Ninh, T.K.T.; Massin, L.; Laurenti, D.; Vrinat, M. A New Approach in the Evaluation of the Support Effect for NiMo Hydrodesulfurization Catalysts. *Applied Catalysis A: General* **2011**, *407*, 29–39, doi:10.1016/j.apcata.2011.08.019.
5. Badoga, S.; Mouli, K.C.; Soni, K.K.; Dalai, A.K.; Adjaye, J. Beneficial Influence of EDTA on the Structure and Catalytic Properties of Sulfided NiMo/SBA-15 Catalysts for Hydrotreating of Light Gas Oil. *Applied Catalysis B: Environmental* **2012**, *125*, 67–84, doi:10.1016/j.apcatb.2012.05.015.
6. Wang, X.; Zhao, Z.; Zheng, P.; Chen, Z.; Duan, A.; Xu, C.; Jiao, J.; Zhang, H.; Cao, Z.; Ge, B. Synthesis of NiMo Catalysts Supported on Mesoporous Al_2O_3 with Different Crystal Forms and Superior Catalytic Performance for the Hydrodesulfurization of Dibenzothiophene and 4,6-Dimethyldibenzothiophene. *Journal of Catalysis* **2016**, *344*, 680–691, doi:10.1016/j.jcat.2016.10.016.
7. Muñoz-López, J.A.; Toledo, J.A.; Escobar, J.; López-Salinas, E. Preparation of Alumina–Titania Nanofibers by a pH-Swing Method. *Catalysis Today* **2008**, *133–135*, 113–119, doi:10.1016/j.cattod.2007.12.044.
8. Obeso–Estrella, R.; Pawelec, B.; Mota, N.; Flores, L.; Melgoza, J.M.Q.; Yocupicio–Gaxiola, R.I.; Zepeda, T.A. Elucidating the Mechanisms of Titanium–Induced Morphological and Structural Changes in Catalysts on Mesoporous Al_2O_3–TiO_x Mixed Oxides: Effect of Non–Stoichiometric TiO_x Phase. *Microporous and Mesoporous Materials* **2022**, *339*, 111991, doi:10.1016/j.micromeso.2022.111991.
9. [9] Vaiano, V.; Iervolino, G.; Sannino, D.; Rizzo, L.; Sarno, G.; Farina, A. Enhanced Photocatalytic Oxidation of Arsenite to Arsenate in Water Solutions by a New Catalyst Based on MoO_x Supported on TiO_2. *Applied Catalysis B: Environmental* **2014**, *160–161*, 247–253, doi:10.1016/j.apcatb.2014.05.034.

10. [10] Dominguez Garcia, E.; Chen, J.; Oliviero, E.; Oliviero, L.; Maugé, F. New Insight into the Support Effect on HDS Catalysts: Evidence for the Role of Mo-Support Interaction on the MoS_2 Slab Morphology. *Applied Catalysis B: Environmental* **2020**, *260*, 117975, doi:10.1016/j.apcatb.2019.117975.
11. Gao, D.; Duan, A.; Zhang, X.; Zhao, Z.; E, H.; Li, J.; Wang, H. Synthesis of NiMo Catalysts Supported on Mesoporous Al-SBA-15 with Different Morphologies and Their Catalytic Performance of DBT HDS. *Applied Catalysis B: Environmental* **2015**, *165*, 269–284, doi:10.1016/j.apcatb.2014.10.034.